九州大学大学院総合理工学報告
第23巻 第2号 197-206頁 平成13年9月

Engineering Sciences Reports, Kyushu University
(KYUSHU DAIGAKU SOGORIKOGAKU HOKOKU)
Vol. 23, No. 2 pp. 197-206 SEPT. 2001

Measurement of Projected Area Factors for Each Part of a Sitting Person

Masayuki OGURO*, Edward ARENS**, Hui ZHANG**
Kazuyo TSUZUKI*** and Tadahisa KATAYAMA****

(Received May 30. 2001)

This paper provides projected area factors for each part of a sitting person to allow the radiative heat transfer between the human and surrounding surfaces to be calculated. We first briefly describe ways of calculating angle factors and effective radiation area for each segment of a sitting person. Then we describe an approach to measuring projected area factors using a manikin. Projected area factor distributions are presented, and then effective radiation area and angle factors are calculated and compared with the results of other studies.

1. Introduction

In the course of designing architecture or evaluating the performance of buildings, thermal comfort for occupants is one of the most important issues. Especially after the invention of air conditioning technology, thermal comfort has been a big issue in designing buildings because it affects not only the comfortableness but also the productivity of workers in buildings. In addition, much of the energy consumption in buildings is for air conditioning, and there are large opportunities to conserve energy through rational air-conditioning design.

There are many situations in buildings where the evaluation of asymmetric thermal radiation environment is required. For example, environments in buildings near cold windows in winter, room environments controlled by heated or cooled panel systems, environments in large spaces like atria which have large temperature gradient between floor and ceilings in addition to many cold/hot windows, and so on. In these highly asymmetric environments, radiation analysis is required not only for the whole body but also for individual body parts. There is a strong need for a radiation analysis model at the body-part level, and for empirical data for the model (Stolwijk[1], 1971, Tanabe[2], 1998 etc.). The completion of such a model partly depends on new radiation analysis and empirical data describing each part of the human body.

There are many studies on evaluation of thermal comfort and heat transfer at the body-part level.[3)~10)] Also there are many studies on projected area for human body.[11)~15)] However there is no study which fully describes all the projected area factors at the body-part level for all directions around the human body so that all the angle factors between any plane and each body part can be estimated. This paper is the second of two describing measurements of projected area factors for each part of the body so that radiation exchange between any surrounding plane and a body part, (or the effect of solar radiation on a human body part), can be calculated. The first paper[21)] describes standing posture, this paper is about seated posture. We first briefly describe ways to calculate angle factors, effective radiation area for each segment of the human body under certain conditions. Then we present measured distribution

*Technology Center, Taisei Corporation
**Center for Environmental Design Research, Univ. of California
***National Institute of Bioscience and Human-technology
****Department of Energy and Environmental Engineering

of projected area factors for 16 body segments. At the end the effective radiation areas and angle factors are calculated and compared with those from other studies.

2. Description of Thermal Radiation

Fanger[15] (1970) measured the projected area factors of a whole human body as seen from all directions, using photographs taken from 7m away, and then calculated the angle factors between the body and the surfaces of a rectangular space. Steinman[16] also calculated angle factors between a whole body and inclined walls using those data. Fanger's data are very useful because no matter what the distance is between a space and the human body, the angle factors can be calculated from the projected area factor distribution. Horikoshi[17),18)] et al. (1978, 1988) and Tsuchikawa[19] et al. (1988) directly measured angle factors between rectangular planes and the human body by photographing at short distances using a special fisheye lens. However all these data can only be used for a whole human body.

For standing posture, Tsuchikawa[20] et al. (1991) measured angle factors between rectangular planes and 4 parts of the human body (head, arms, trunk, and legs), using a fisheye lens from distances of 1 to 2.5 meters. However their angle factor diagrams can only be used in those distances.

In this study we took Fanger's approach[15] to estimate angle factors from measured projected areas, because angle factors can be calculated no matter what the distance is. We did this for each body part individually; the whole body values can then be obtained by summing the parts.

2.1 Angle factor between a body part and a plane

Consider a man and a plane in the surrounding with a surface area A_2. Consider one of the body parts with effective radiation area A_1 and a differential element dA_2 out of the plane. Imagine the connecting line from the center of the body part to the center of dA_2. If the size of the body part A_1 and the portion dA_2 is very small compared to the distance between them the angle factor between them can be calculated as follows. (Oguro[21], 2001)

$$F_{1-A2}=(1/\pi)\int_{A2}\{(f_P/R^2)\cos\theta_2\}dA_2 \quad (1)$$

$$f_P=(A_P/A_1) \quad (2)$$

Where,

F_{1-A2} : Angle factor between A_1 and dA_2

f_P : projected area factor

R : distance between A_1 and dA_2

A_1 : effective surface area of the targeted body part

A_2 : surface area of the plane

dA_2 : differential surface area of the plane

θ_2 : polar angle (angle of incidence) between the connecting line of the center of the two differential surfaces and the normal of differential surface dA_1

A_p : the projected area of the body part on the half sphere with radius of R whose center is at the center of dA_2

Using Eq. (1), once fp distribution against all the directions is determined, any angle factor from a body part A_1 to any surface A_2 can be determined through numerical integration.

2.2 Effective radiation area

Consider a large sphere with radius r instead of the plane A_2. Because F_{1-A2} should be 1.0, the effective radiation area of the body part A_1 can be estimated from Eq. (3).

$$A_1=(1/\pi)\int_{A2}\{(A_P/R_r^2)\cos\theta_r\}dA_r \quad (3)$$

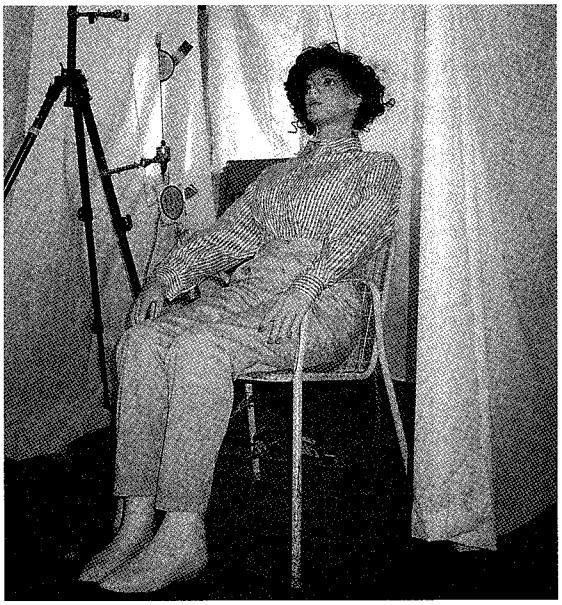

Fig. 1 Thermal manikin

Table 1 Surface areas

Body Segment	Surface Area(㎡)	Body Segment	Surface Area(㎡)
Back	0.128	Left Thigh	0.160
Chest	0.138	Right Arm	0.051
Head	0.117	Right Foot	0.042
Left Arm	0.050	Right Hand	0.036
Left Foot	0.043	Right Leg	0.090
Left Hand	0.038	Right Upper Arm	0.073
Left Leg	0.090	Right Thigh	0.166
Left Upper Arm	0.076	Pelvic Region	0.170
Total 1.469 (㎡)			

$$f_{eff}=A_1/A_m \tag{4}$$

Where,

dA_r : differential area on the sphere with radius Rr from which solid angles are measured.

R_r : the distance between targeted part A_1 and dA_r

θ_r : polar angle on dA_r

f_{eff} : effective radiation area factor for part A_1

A_m : actual surface area of part A_1

Using (3), once Ap distribution against all the directions is determined we can estimate the effective radiation area A_1. This effective radiation area estimation is needed only once for each posture of the human body. By considering the body part as the whole human body, Eq. (1) through Eq. (4) can be used also for the whole human body.

3. Measurement of Projected Area Factors

3.1 Thermal Manikin

A segmented thermal manikin (Tanabe, [22]1994) was used for the measurement of projected area of the human body segments. This manikin, of female shape, is one of several developed to evaluate asymmetric thermal environment by measuring the heat loss at each part of the body. **Fig.1** shows a picture of the thermal manikin. The 16 body segments and their respective surface areas are listed in **Table 1**. The manikin was chosen for the radiation study based on the following considerations:

a .The surface area of each segment is clearly defined.

b .Combination of heat loss measurement and this radiation study enables us to separate radiative and convective heat transfer.[3),4)]

c .There is almost no limitation concerning measurement procedure.

3.2 Measurement procedure

A sky simulator dome of radius 3.5m was used for this radiation study. The facility has a guide rail running longitudinally to the zenith. In normal use, a light representing the sun travels up and down this rail on a motorized carriage. A turntable at the base of the half sphere allows the sun's azimuthal movement to be simulated. By setting a camera instead of the light bulb on the carriage and

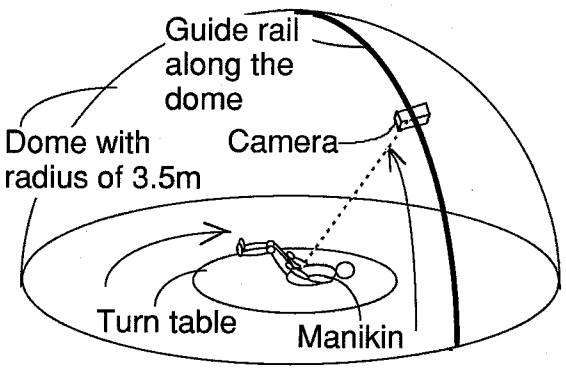

Fig. 2 Experimental set-up for projected area measurement

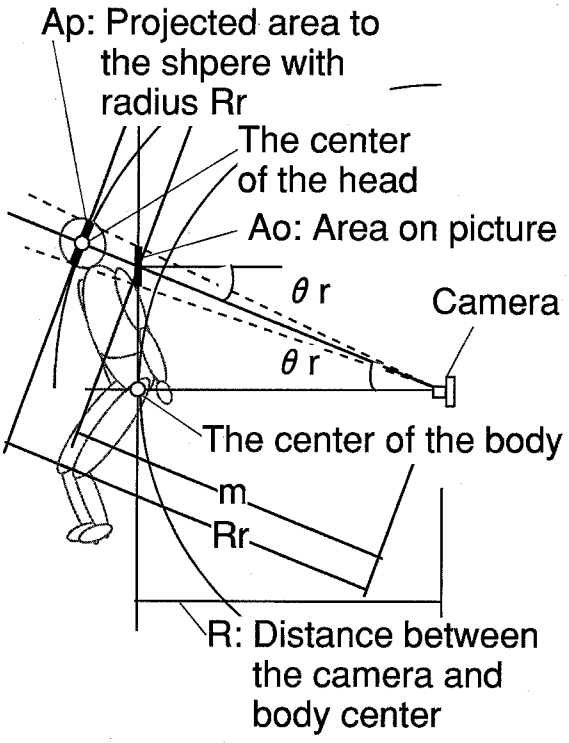

Fig. 3 Estimation of projected area factors of a segment from pictures taken toward body center

laying the manikin on the turntable, one can easily take pictures from all directions. **Fig.2** is the experimental set-up for measuring the manikin's projected areas. The manikin's posture is sitting. First the manikin was set on her back on the turntable and rotated in the horizontal plane. In order to set the manikin securely on the turntable, there is 30 degrees of inclination between the vertical axis for actual sitting posture and the plane of the turntable. Pictures were taken with a 35mm camera with a 50mm lens. For 0, 15, 30, 45 degrees vertical angle, pictures were taken at every 15 degrees in horizontal angle. For 60 and 75 degrees vertical, pictures were taken every 30 degrees in horizontal angle. One picture was taken at 90 degrees. After recording the pictures with the manikin on her back, the manikin was turned over and set face-down. Then the above-mentioned procedure was repeated. The center of the pelvic region was set at the center of the dome throughout the experiment. The center of the body was 0.50m above the floor for the sitting manikin.

In addition, pictures of a ball with radius of 239mm were taken in order to determine the conversion ratio from the negative area (measured in number of pixels) to the actual area in square meters.

3.3 Estimation of projected area

All the films were developed and the negatives were used to analyze projected areas. The negatives were digitized at 1000 dots per inch resolution. The number of pixels was counted by using computer software (SigmaScan 2.00) for image measurement.

The conversion ratio from pixels to actual projected area was estimated by dividing the known projected area of the ball by the number of the pixels in its photograph. This conversion ratio was used for all the picture analyses. The areas estimated in the above manner correspond to the area on the plane normal to the direction of the camera at the distance of 3.5m. Thus the areas further away have to be converted to the required projected areas at the position of each segment. For this purpose the coordinates for each segment of the body were also measured from the pictures taken from the top of the dome and in the horizontal plane. **Fig. 3** shows the relationship between projected area A_p and the area estimated from counting the number of pixels. A_p can be estimated as follows.

$$A_p = A_0 (m/R_r)^2 \cos\theta_r \quad (5)$$

Where,

A_0 : the area on the plane normal to the direction of the camera at the distance of 3.5m
m : the distance between the A_0 and the camera
R_r : the distance between targeted part and the camera
θ_r : polar angle on dA_0

4. Results and Discussion

Fig. 4 shows the orthogonal coordinate system for the segment of the body and the spherical coordinate system for projected area distribution. As we stated before, in order to set the manikin securely on the turntable, there is a 30 degrees of inclination between the vertical axis for sitting posture and the plane of the turntable. This means that the angle between the Z-axis in the orthogonal coordinate system and the plane for angle A in spherical coordinate system in this study is 30 degrees. The measured locations for each part of the body are shown in **Table 2** in the orthogonal coordinate system. The conversion ratio of actual area to the number of pixels is 0.0228 square centimeters per pixel. Projected area factors are presented in the spherical coordinate system. For the upper arm, arm, hand, thigh, leg, and foot, only left side of the body were analyzed, and in the following analyses the same fp distribution are assumed for the right side of the body.

4.1 Effective radiation areas and effective radiation area factors

First the projected area distributions were acquired, and then numerical integration based on Eq. (3) was carried out. The calculated effective radiation areas and the effective radiation area factors for the whole body are listed in **Table 3**, compared with the results from other studies. The total body effective radiation area factor in this study is 0.80 a larger value than those in the other studies. This may be due to a slight difference of sitting posture, i.e., the posture of the manikin in this study may be slightly more open-legged and reclined than the others. The results for each part of the body are listed in **Table 4**, and compared with Ozeki's results. When comparing head and arms, the ratios of these parts to the total are consistent with the Ozeki's results. The differences of about 6% in body and 15% in legs may be due to the difference of the line dividing the body and legs and the position of legs. The largest effective radiation areas, in order, are the pelvic region, thighs, back, and

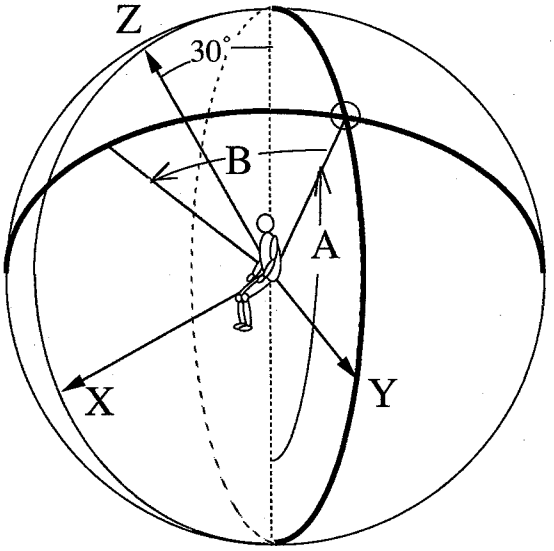

Fig. 4 Coordinate system

Table 2 Coordinates of segments

Body Segment	Coordinates (m)			Body Segment	Coordinates (m)		
	X	Y	Z		X	Y	Z
Back	−0.04	0.00	0.41	Left Thigh	0.10	0.11	−0.05
Chest	0.13	0.00	0.37	Right Arm	0.19	−0.23	0.18
Head	0.13	0.00	0.70	Right Foot	0.18	−0.07	−0.60
Left Arm	0.17	0.24	0.17	Right Hand	0.33	−0.22	0.00
Left Foot	0.12	0.06	−0.59	Right Leg	0.26	−0.09	−0.37
Left Hand	0.29	0.28	−0.02	Right Upper Arm	0.06	−0.22	0.30
Left Leg	0.19	0.08	−0.39	Right Thigh	0.11	−0.10	−0.03
Left Upper Arm	0.06	0.21	0.41	Pelvic Region	0.00	0.00	0.11

Table 3 Comparison of effective radiation area factors for whole human body

	Present Study	Fanger et al. [15]	Tsuchikawa et al. [19]	Tsuchikawa et al. [20]	Ozeki et al. [5]	Miyazaki et al. [7]
Height(m)	1.60	1.72	1.63	1.64	1.75	1.71
Surface Area(㎡)	1.47	1.74*	1.51*	1.57*	1.72	1.58
Eff. Rad. Area(㎡)	1.18	1.21	1.13	1.12	1.18	1.22
Eff. Rad. Area Factor(—)	0.80	0.70	0.75	0.71	0.69	0.78

*DuBois Area

Table 4 Comparison of effective radiation areas

Body Segment	Eff. Rad. Area(㎡) Present Study	Body Segment	Eff. Rad. Area(㎡) Present Study	Eff. Rad. Area(㎡) Ozeki et al. [5]
Back	0.123	Head	0.11 9%	0.12 10%
Chest	0.108			
Head	0.105			
Left Arm	0.040			
Left Foot	0.036	Body (Back & Chest & Pelvic Region)	0.38 32%	0.45 38%
Left Hand	0.029			
Left Leg	0.076			
Left Upper Arm	0.061			
Left Thigh	0.126	Arms (Arms & Upper Arms & Hands)	0.26 22%	0.29 25%
Right Arm	0.040			
Right Foot	0.035			
Right Hand	0.028			
Right Leg	0.076	Legs (Feet & Legs & Thighs)	0.48 41%	0.31 26%
Right Upper Arm	0.059			
Right Thigh	0.131			
Pelvic Region	0.145			
Total	1.217		1.22 103%	— —
Whole Body	1.177		1.18 100%	1.17 100%
Surface Area			1.47	1.72

Table 5 Effective radiation area factors

Body Segment	Eff. Rad. Area Factor	Body Segment	Eff. Rad. Area Factor
Back	0.96	Left Thigh	0.79
Chest	0.78	Right Arm	0.80
Head	0.90	Right Foot	0.83
Left Arm	0.80	Right Hand	0.77
Left Foot	0.83	Right Leg	0.84
Left Hand	0.77	Right Upper Arm	0.80
Left Leg	0.84	Right Thigh	0.79
Left Upper Arm	0.80	Pelvic Region	0.86
Whole Body 0.80			

chest. The actual surface areas of back and chest are in the opposite order. This is because the effective radiation area of the chest is decreased by its view of the thighs which block radiation exchange with some of the lower surroundings. The effective radiation area factors based on Eq. (4) are also listed in **Table 5**. The effective radiation area factors of the hands and arms are a little less than other segments. This can be explained by blocking effect of the trunk that exists along those segments.

4.2 Projected area distribution

Eq. (2) gives us the projected area factors, and these enable us to calculate angle factors from each part of the body to any plane. **Fig. 5** shows the results of the distribution of the projected area factor for the whole human body. Concerning whole-body results, the distribution is symmetrical between A <180° and A> 180° as might be expected. However symmetry cannot be seen between the front side and back side, as expected.

Fig. 6(a) and **6(b)** show the results of the distribution of projected area factors for each segment. For example, in the left arm we can understand that the left arm can not be seen from her front side because it is almost perfectly blocked by other body parts when A is 180° to 315° and B is −15° and −30° . When comparing between the front side and back side, basically any segment that is part of a limbs cannot have a symmetrical distribution between the front side and back side. This can be explained in that some of them are blocked by a different segment when seen from the front side versus

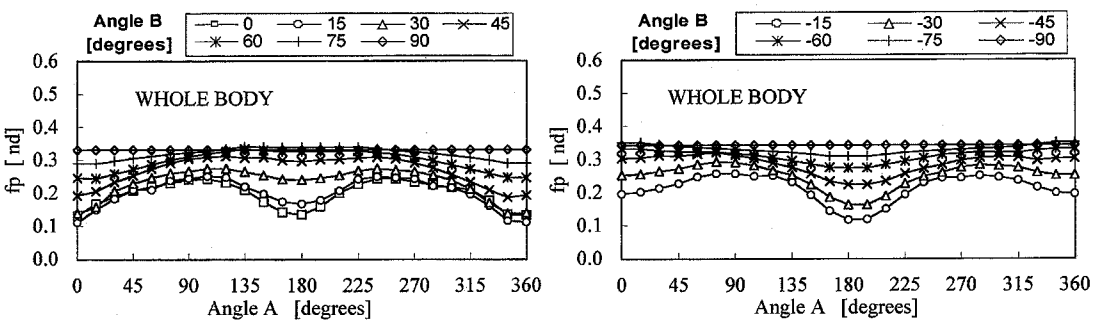

Fig. 5 Projected area factor distribution for WHOLE BODY

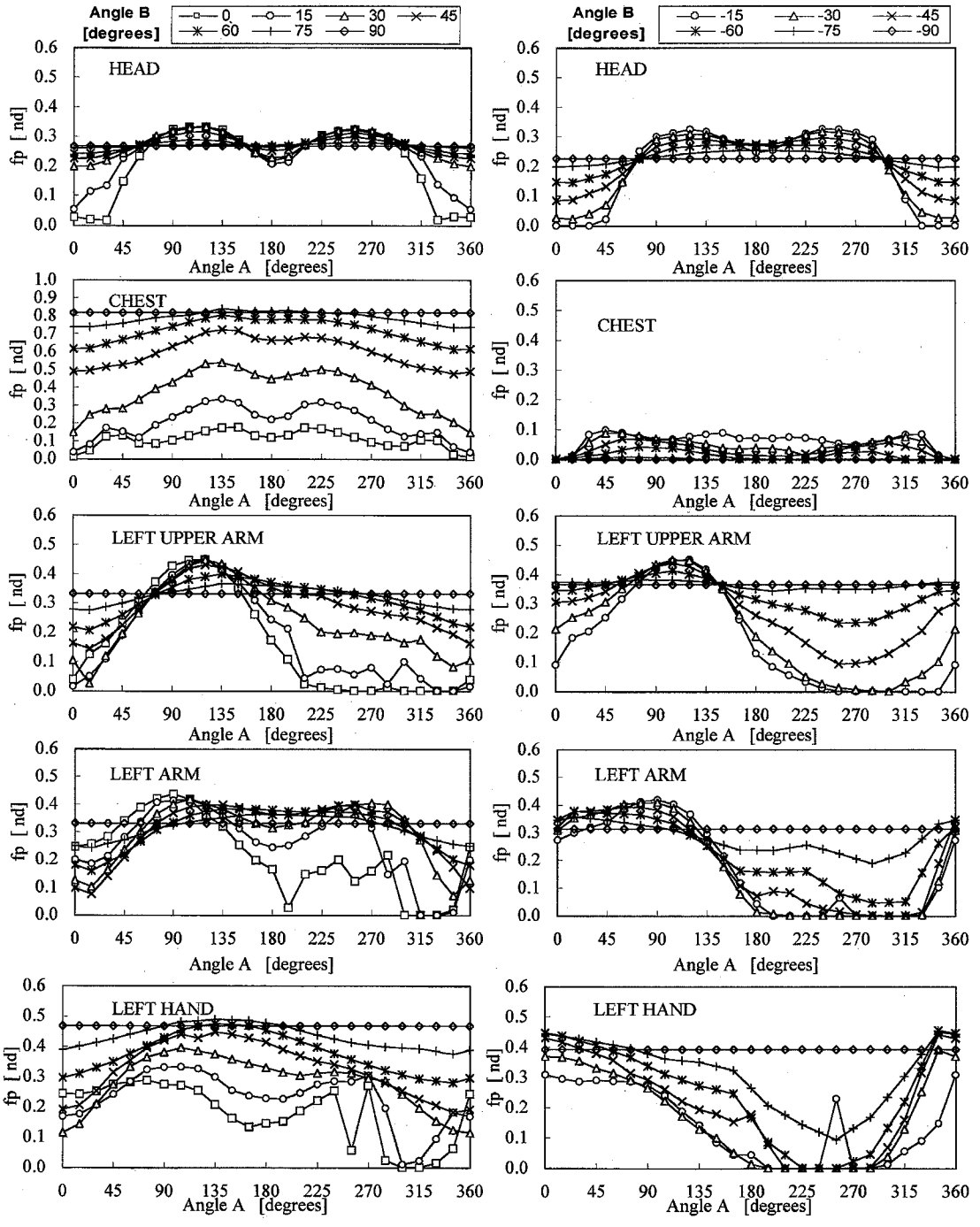

Fig. 6 (a) Projected area factor distribution for each part

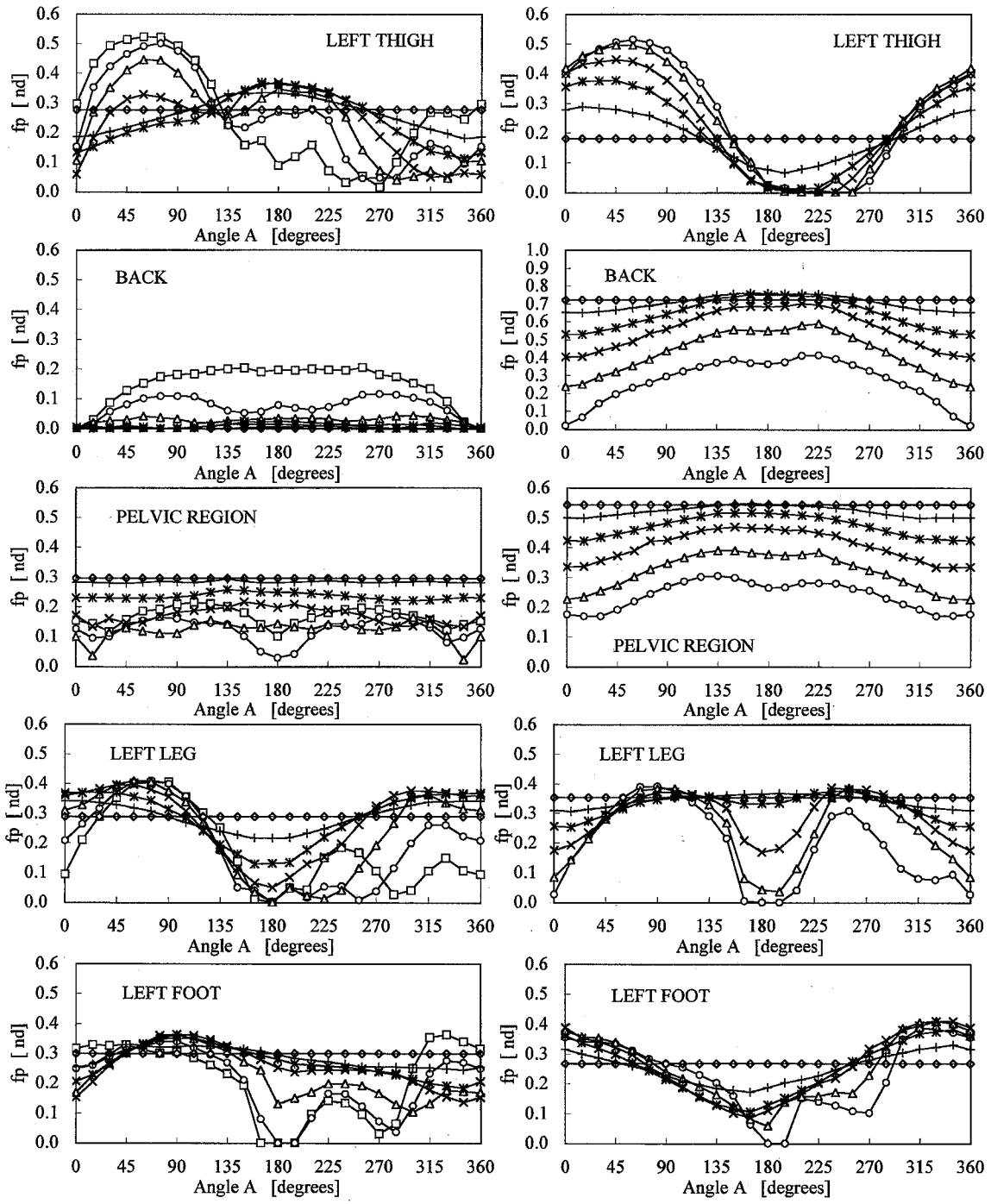

Fig. 6 (b) Projected area factor distribution for each part

from the back side. Some of them also have different shapes from the front and back because of the slope of the lines dividing the segments of the whole body.

4.3 Angle factor for whole body

Based on Eq. (1), angle factors between the sitting person and a rectangle were calculated for a comparison with Fanger's and Tsuchikawa's results. **Fig. 7** shows the results for the whole body with Fanger's data. The difference was very small in the case of side walls. Considering the difference of height of his subjects versus the manikin (172/160 centimeters), the side wall results are in very good agreement. On the other hand, in the case of front walls or ceilings, significant differences can be seen. This may be due to the difference of their posture, i.e., the posture in this study is more

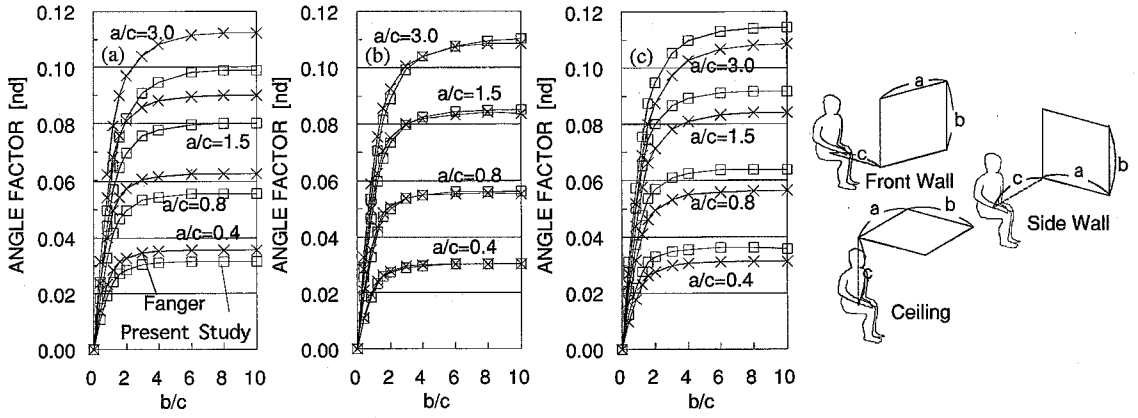

Fig. 7 Comparison of angle factor with Fanger's results for (a) front walls, (b) for side walls, (c) for ceilings.

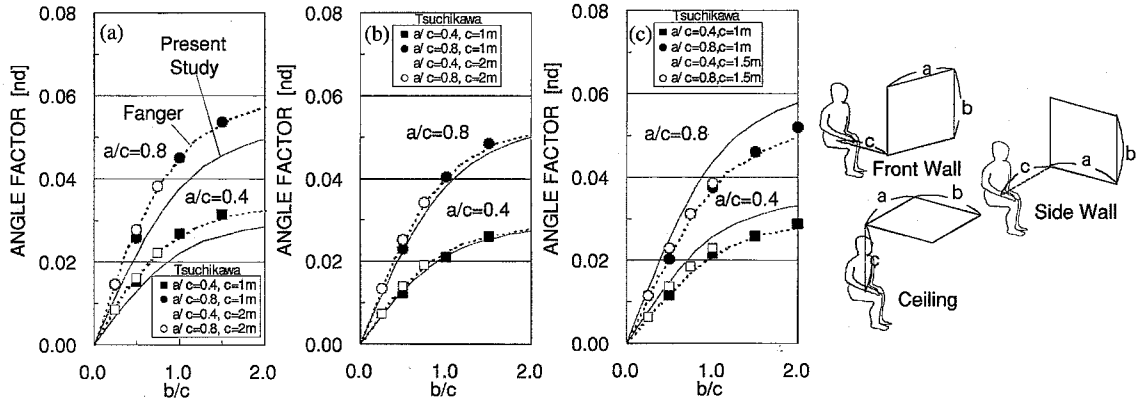

Fig. 8 Comparison of angle factor in short distances for (a) front walls, (b) for side walls, (c) for ceilings.

open and reclined toward the back of the chair than that in Fanger's study. **Fig. 8** shows the comparison with Tsuchikawa's results for short distances. For side walls, in considering the difference of height of their subject and our manikin (167.7/160 centimeters), the results are also in very good agreement. These results suggest that our data can be used for side walls even for short distances. On the other hand, our results are significantly different from Tsuchikawa's results for front walls and ceilings. Fanger's data are in good agreement with Tsuchikawa's data. A reasonable conclusion on the use of those data for sitting posture would be that our data, Tsuchikawa's data and Fanger's data could be used both for near and distant walls, but the effect of the difference of the posture, i.e., reclined or not, could result in significant difference in angle factors, especially for front walls and ceilings.

5. Summary

We measured the projected area factors for each part of a sitting person by using a sitting thermal manikin. Effective radiation area and angle factors were calculated from these measured data and compared with whole-body values obtained in other studies. The comparison generally shows good agreement and for both distant or near walls and ceilings. The projected area factors for each body part measured in this study can be used in many ways to investigate radiation heat transfer between each part of a sitting person and its surroundings.

References

1) J. A. J. Stolwijk, NASA, CR-1855, 1971.
2) S. Tanabe, S. Horikawa, M. Kin, H. Tsutumi, Proceedings of SHASE, pp. 989-992, 1998.
3) R. deDear, E. Arens, H. Zhang, M. Oguro, International Journal of Bio meteorology, Vol. 40, No. 3, pp. 141-156, 1997.
4) M. Ichihara, M. Saitou, M. Nishimura, S. Tanabe, Journal of Architectural Planning and Environmental Engineering, AIJ, No. 501, pp.45-51, 1997.
5) Y. Ozeki, M. Konishi, C. Narita, Y. Kurazumi, S. Tanabe, Journal of Architectural Planning and Environmental Engineering, AIJ, No. 522, pp. 15-22, 1999.
6) K. Suzuki, N. Kakitsuba, Journal of Architectural Planning and Environmental Engineering, AIJ, No. 515, pp. 49-55, 1999.
7) Y. Miyazaki, M. Saito, Y. Seshimo, Journal of Human and Living Environment, No. 1, pp. 92-100, 1995.
8) J. Ishii, T. Horikoshi, S. Watanabe, K. Suzuki, Y. C. Zhi, Journal of Architectural Planning and Environmental Engineering, AIJ, No. 530, pp. 31-37, 2000.
9) T. Horikoshi, T. Tsuchikawa, Y. Kurazumi, K. Hirayama, Y. Kobayashi, Journal of Architectural Planning and Environmental Engineering, AIJ, No. 413, pp. 21-28, 1990.
10) T. Miyanaga, W. Urabe, Y. Nakano, A. Hoyano, Journal of Architectural Planning and Environmental Engineering, AIJ, No. 526, pp. 51-58, 1999.
11) W. Underwood, Ergonomics, pp. 155-168, 1966.
12) Y. Ozeki, . Konishi, C. Narita, Y. Kurazumi, S. Tanabe, Journal of Architectural Planning and Environmental Engineering, AIJ, No. 525, pp. 45-51, 1999.
13) S. Miyamoto, T. Horikoshi, Y. Hirokawa, Journal of Architectural Planning and Environmental Engineering, AIJ, No. 513, pp. 47-52, 1998.
14) A. Tomita, S. Miyamoto, T. Horikoshi, Journal of Architectural Planning and Environmental Engineering, AIJ, No. 518, pp. 7-12, 1999.
15) P.O. Fanger, O. Angelius, P. Kjerulf-Jensen, ASHRAE Transactions, Vol. 76, pp. 338-373, 1970.
16) M. Steinman, L. N. Kalisperis, L. H. Summers, ASHRAE Transactions, Vol. 76, pp.1809-1823, 1988.
17) T. Horikoshi, H. Miyahara, Y. Kobayashi, Transaction of AIJ, No. 268, pp. 109-119, 1978.
18) T. Horikoshi, Y. Kobayashi, Transaction of AIJ, No. 322, pp. 92-99, 1982.
19) T. Tsuchikawa, T. Horikoshi, E. Miwa, Y. Kurazumi, K. Hirayama, Y. Kobayashi, Journal of Architectural Planning and Environmental Engineering, AIJ, No. 388, pp. 48-45, 1988.
20) T. Tsuchikawa, T. Horikoshi, E. Kondo, Y. Kurazumi, K. Hirayama, Y. Kobayashi, Journal of Architectural Planning and Environmental Engineering, AIJ, No. 428, pp. 67-75, 1991.
21) M. Oguro, E. Arens, H. Zhang, K. Tsuzuki, T. Katayama, to be published in Journal of Architectural Planning and Environmental Engineering, AIJ, Sept. 2001.
22) S. Tanabe, E. Arens, F. Bauman, H. Zhang, M, T. Madsen, ASHRAE Transactions, Vol. 100, 1994.